Solid Freeform Fabrication 2018: Proceedings of the 29th Annual International Solid Freeform Fabrication Symposium – An Additive Manufacturing Conference
Reviewed Paper

Aligning Material Extrusion Direction with Mechanical Stress via 5-Axis Tool Paths

J. A. Gardner*, T. Nethercott-Garabet*, N. Kaill*, R. I. Campbell, G. A. Bingham*, D. S. Engstrøm^, and N.O. Balc[+]

*Loughborough Design School, Loughborough University, United Kingdom
^Wolfson School of Engineering, Loughborough University, United Kingdom
[+]Department of Manufacturing Engineering, Technical University of Cluj-Napoca, Romania

Abstract

Mechanical properties of parts fabricated via the Material Extrusion (ME) process can be improved by optimising process settings, however, their properties are strongly influenced by build orientation due to the stair-stepping effect initiating cracks whilst under load. 5-axis ME enables the fabrication of parts without the layer-by-layer restrictions that conventional 3-axis strategies impose. By aligning extrusion direction with high stress tensors, 5-axis tool paths can be used to reduce the effects of weak inter-layer bonds.

To establish performance differences between parts manufactured by either strategy, wave spring-inspired geometry was selected for production, due to the multi-directional tensile loads acting throughout the material. 5-axis and 3-axis tool paths were generated via the Grasshopper 3D virtual environment within Rhinoceros 3D and MakerBot Desktop, and manufactured using a 5AXISMAKER and a MakerBot Replicator 2, respectively. To evaluate performance differences between the two strategies, compression tests were conducted on the parts.

Keywords: Additive Manufacturing, 5-axis, Tool path, Material Extrusion, G-code

Introduction

Material Extrusion (ME) is an Additive Manufacturing (AM) process category in which material (usually a thermoplastic polymer) is heated and extruded onto a substrate. The semi-molten filament forms a partial bond with previously deposited material, cools, and solidifies to form a layer of material [1]. The unique capability of AM typically relies on the translation of Computer-Aided Design (CAD) geometry into Two-Dimensional (2D) cross-sectional areas which are then successively fabricated, layer-by-layer to produce near net shape parts. By adopting a layer-by-layer strategy, complex, multi-functional parts can be fabricated, minimising the waste, tooling, and fixtures associated with conventional manufacturing methods [2]. Despite these advantages, there are fundamental AM process limitations preventing its wide-scale adoption across manufacturing industry. Many of these limitations occur from the build-up of layers, namely: loss of dimensional accuracy, stair-stepping effect (leading to poor surface finish), and anisotropic mechanical properties. These limitations are especially problematic within ME for the manufacture of thin-walled, or curved surfaces [3]. Mechanical instability within ME parts is strongly influenced by reduced bond strength between successive layers. Also, because the polymer is only partially melted, full part density often cannot be achieved [4]. Additionally, the rapid heating of the polymer through the nozzle followed by cooling causes a

phase change in the material resulting in volumetric shrinkage of the filament bead. This can cause warpage, internal stress, and porosity between filaments, thus reducing the strength of a part [5, 6]. ME parts can be described as an anisotropic composite of discontinuous polymer fibres and voids [7]. Within the context of producing complex functional end-use parts, ME is caught in a paradoxical scenario in which layer-by-layer fabrication is both its greatest enabler and limiting factor.

The objective of this research was to investigate a novel AM process based on ME which uses 5-axis Computer Numerical Control (CNC) tool paths to deposit material in a non-planar strategy. It was envisioned that altering the orthotropic accumulation of layers to a dynamic 3D accumulation, parts would exhibit: more consistent material properties, greater surface contact area between each 'layer', and improved surface finish, thus improving mechanical performance and predictability when compared with 3-axis built equivalents. This process could enable the fabrication of low cost, customisable, parts with properties suitable for end use, load-bearing applications.

Several 5-axis controlled AM processes are commercially available, for example, they are often used within direct energy deposition; a form of laser welding. Whereas conventional 3-axis AM strategies slice geometry into simplified 2D tool paths, 5-axis tool path generation becomes dynamic, requiring specialist software not usually associated with AM. Curved layer Material Extrusion (CLME) is an AM process which has been developed over the past decade and presented by a number of authors [3, 4, 8]. A ME machine is typically modified with an additional axis of rotational movement in the substrate allowing the tool movement required to deposit curved layers. Singameni et al. [7] compared the mechanical properties of ABS parts manufactured using regular 3-axis material extrusion and 4-axis CLME. It was found that curved-layer parts had a superior mechanical performance. The average maximum load until failure increased by 40% during a non-standard bending test. Surface finish of the curved layer parts was also improved since no 'stair-stepping' effect was observed, reducing the chance of cracks initiating at surface irregularities. Additionally, it was observed that the curved layers prevented crack propagation, delaying catastrophic failure of the samples.

Method

To compare the mechanical properties between parts built with 5-axis and 3-axis machine configurations, wave spring-inspired geometries, hereon referred to as 'wave springs' for simplicity, were fabricated in PLA. Non-standard mechanical compression tests were then conducted on each sample.

For a wave spring in axial compression, an estimation of deflection (Eq.1.) and operating stress (Eq.2.) can be calculated using wave spring formula, where: P = load, E = tensile modulus of material, K = multiple wave factor, Dm = mean diameter of spring, Z = number of layers, b = Radial width, t = thickness, and, N = number of waves p/layer. See Figure 1.

$$Deflection = f = \frac{PKD_m{}^3 Z}{Ebt^3 N^4} \frac{I.D}{O.D} \quad , \quad E = \frac{PKD_m{}^3 Z}{fbt^3 N^4} \frac{I.D}{O.D} \tag{1}$$

$$Operating\ Stress = \sigma_{op} = \frac{3\pi P D_m}{4bt^2 N^2} \tag{2}$$

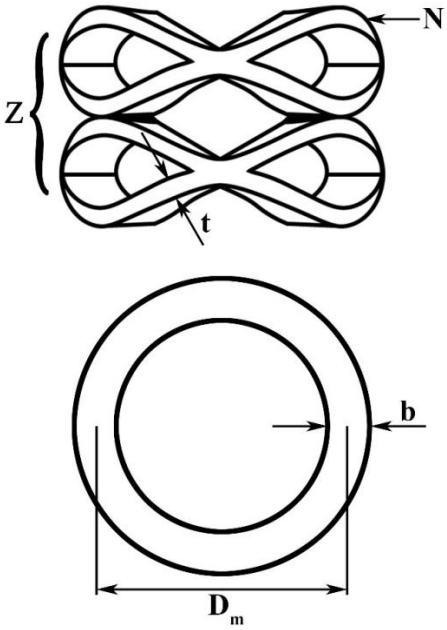

Figure 1 - Wave spring geometry

It is widely reported that build orientation influences elastic modulus and ultimate tensile strength of ME materials [9, 10]. In a material specification sheet for PLA, Stratasys report a 20% reduction in the value of the elastic modulus and a 50% reduction in ultimate tensile stress depending on build orientation [11].

The wave spring formula assumes the spring has homogeneous, isotropic material properties and therefore cannot be accurately applied to 3-axis ME parts since the part could fail at a considerably lower load, due to inter-layer shear exceeding the ultimate shear strength of the material. It was envisioned that building up 3D shells, rather than '2.5' layers, to achieve a final geometry would increase the maximum load of the spring in compression when compared to samples fabricated via conventional 3-axis AM. Additionally, as no inter-layer shear would occur the wave spring formula could be applied.

5-Axis G-code Considerations and Generation

ME of a Computer-Aided Design (CAD) model requires software-based processes to generate commands, or G-code, which are translated by a CNC machine controller into machine movement. Conventional ME machines operate in X, Y, and Z axes and typically build parts via series of one or two axes movements. An interpretation of 3D volumes as multiple, stacked 2D areas allows for the discrete, layer-by-layer generation of G-Code.

The planar nature of 3-axis ME allows for many of the associated G-code generation processes to be automated, therefore requiring minimal user input. Volumetric meshes are imported into virtual environments, process settings are selected, and 3-axis G-code is generated without further user involvement. The authors are unaware of any currently available software able to generate G-code that describes a 5-axis tool path immediately following a mesh import

process. A new process order was therefore required. It was proposed that the initial creation of a tool path could precede the generation of G-code for 5-axis ME.

In all forms of ME, parallel tracks are essential in limiting the variation of surface contact areas between adjacent tracks, as deviations from uniformity may cause bonding issues. Adjacent tracks that are too distant share reduced surface contact areas, whereas tracks too close to one another may cause nozzle blockages due to increased pressures within the extruder assembly. To avoid these problems distances between adjacent tracks were made constant; therefore track sections were designed to be parallel. 2D and 3D parallel tracks are shown in Figure 2a and Figure 2b, respectively.

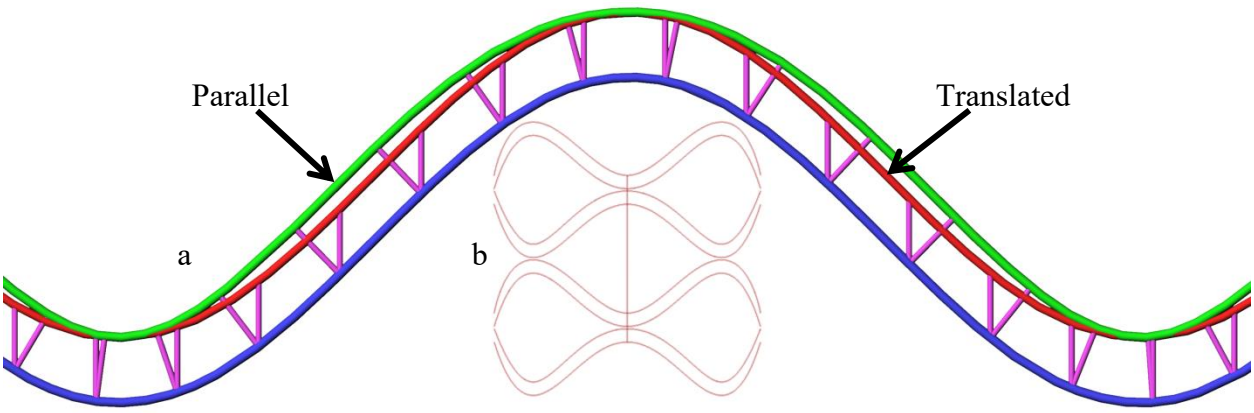

Figure 2 - A comparison of (a) a parallel curve and a translated curve, with equal-length distance indicators, and (b) an example 3D curve created by the developed component cluster

Figure 2a shows that larger angles between the curve's translation direction and its normal vectors increases the distance between the translated and parallel curves. This is a geometry-based consideration rather than a direct G-code-based consideration; however, it was necessary to account for this whilst creating the 5-axis tool paths to reduce the chance of a build failure.

5-axis ME requires new G-code generation methods to: (i) orientate a nozzle to be perpendicular to its travel direction, and; (ii) offset the nozzle tip from obstacles such as jigs and previously extruded material. Additional challenges are also present, such as extruding low-viscosity material through a nozzle not aligned with gravitational forces, and the addition of cooling fans increasing the potential for machine-part collision. These challenges can be addressed by the optimisation of process parameters and by improving system design.

The reference position of a 3-axis ME system can be located at a nozzle tip centre (NTC) as there are no rotating axes to calculate for. Less logic is required to define a reference position that is not affected by rotation, in comparison to defining a position that is affected by rotation. Therefore, 5-axis G-code generation includes constant offsets in the B and C axes to calculate coordinate values for X, Y, and Z.

The 5-axis hybrid manufacturing machine, 5AXISMAKER, was controlled by Mach3 software [12], a G-code reader and executer. To generate the commands an open-source

algorithm [13] was used in Grasshopper 3D [14] within Rhinoceros 3D software [15]. To create the points that the NTC of the 5-axis machine moved between, the open-source algorithm required a single reference curve to describe all its positions.

The creation of the curve, or tool path, was completed via the following steps. A series of points that described a circle were offset from a plane, whereby each point was independently translated by referencing: its index position in the series, a sinusoidal function, the selected wave amplitude, and the selected number of peaks in a layer, all within a component cluster developed by the authors (shown in Figure 3). These translated points were interpolated to create a closed sinusoidal waveform. This curve was subsequently recreated to form a set of parallel curves, which defined a complete wave spring layer. The distance between adjacent curves was calculated by dividing the layer thickness by the number of tracks in the layer. To form a complete shell, copies of the tracks were rotated and translated, according to the selected: number of layers, number of peaks, wave amplitude, offset between layers, and layer thickness (also shown in Figure 3). The shell was then non-uniformly scaled with increasingly larger diameters according to the selected number of shells and shell gap.

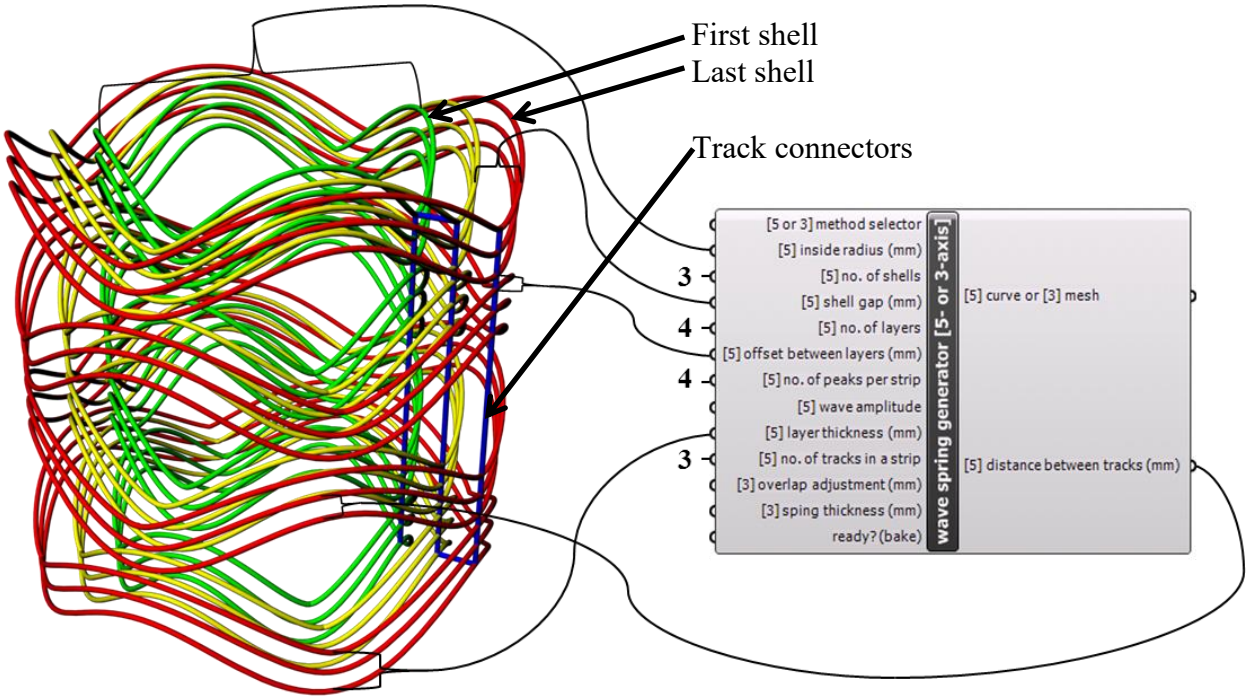

Figure 3 - The developed component cluster with a corresponding tool path showing the relationships between parameter input and output values

At this stage of the G-code generation process all curves, or tracks, were disconnected and required connecting to form a single tool path. To determine how each curve was connected to its neighbour, the 5-axis machine setup was considered. The cables that connected the electronics box to the extruder assembly were located externally from the central column; therefore it was important to consider potential cable entanglement issues. To minimise the probability of entanglement issues and to reduce build time, the completion of each track was

followed by the subsequent track being followed in the reversed direction, as shown schematically in Figure 4.

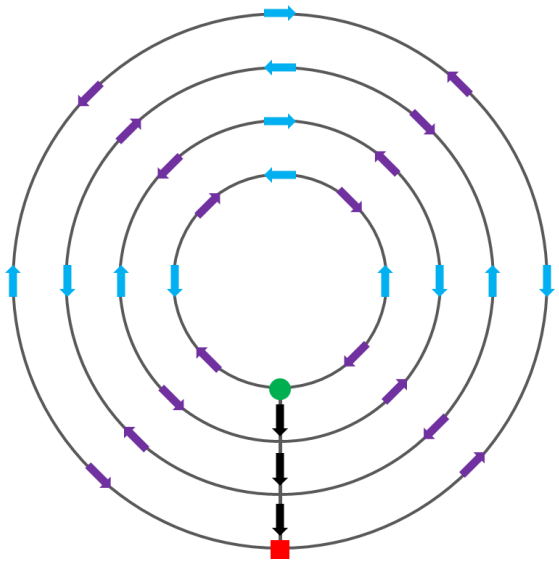

Figure 4 - A top view schematic of the tool path direction

As multiple bimodal parameters were used to determine the direction of the central column, it was important to understand the relationships between the parameters and the directions of each track. The parameters were: the number of tracks in a layer, the number of layers in a shell, and the number of shells in a part (as shown in Figure 3). A flowchart (Figure 5) also displays the top-level logic that was followed to determine track direction.

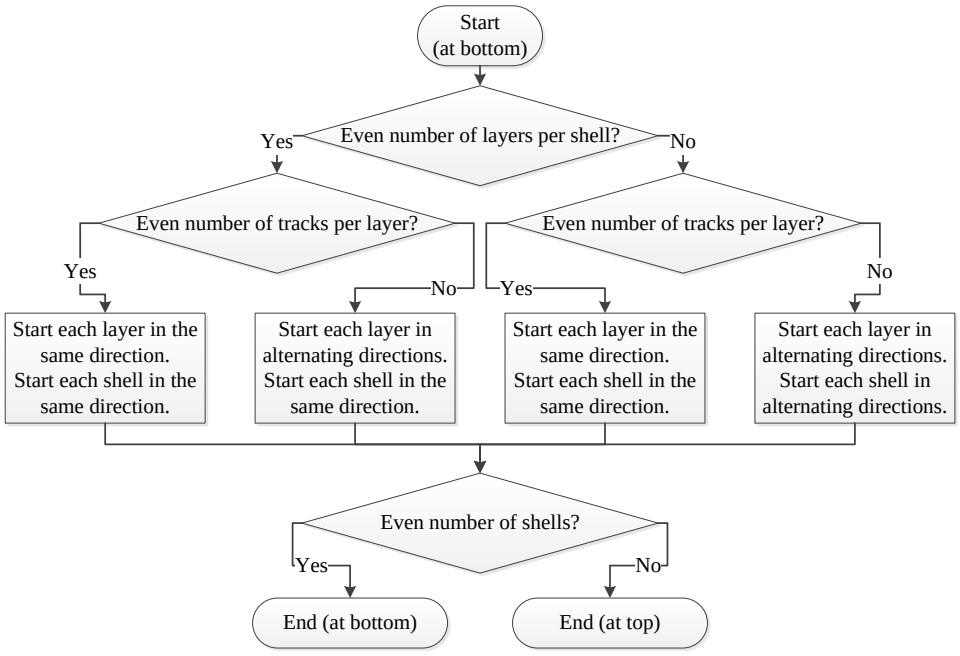

Figure 5 - A flowchart to determine tool path direction to avoid cable entanglement of the 5-axis machine

From the initial movement-based command of 5-axis G-code a sinusoidal wave was built onto a cylindrical jig. Once the first wave was built the nozzle translated in the Z direction only, and then completed the subsequent track in the reversed direction. The number of tracks per layer and the number of layers per shell were calculated by the values of the input variables of the developed component cluster. The values of these bimodal parameters therefore determined the starting direction of each successive layer and shell. The directions of alternating tracks were then reversed, according to logic described in Figure 5, and straight line connectors (shown in Figure 3) were added to connect the end of one track to the beginning of the next. The purpose of this process was to combine a series of tracks into a continious track, allowing the open-source algorithm to calculate all lines of G-code. An example of a complete tool path track can be seen in Figure 6.

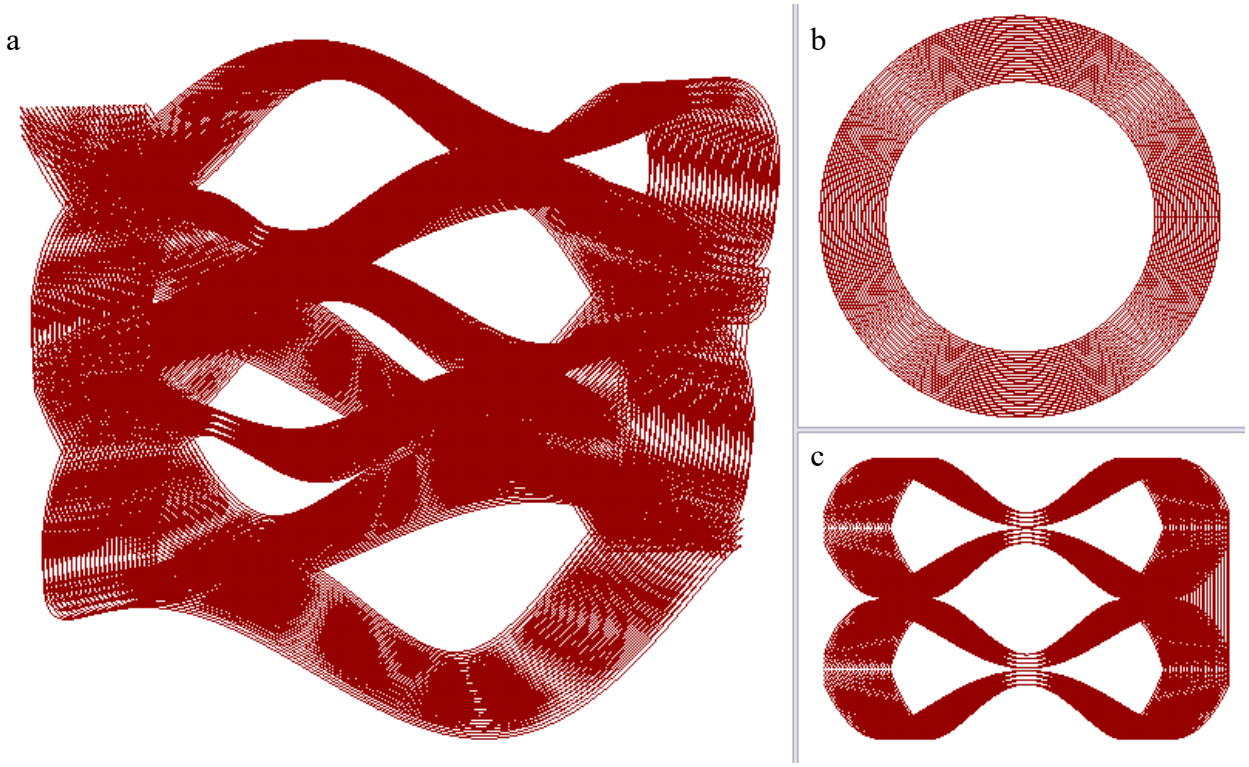

Figure 6 - (a) Perspective, (b) top, and (c) front views of a single curve that represents a wave spring

The tool path curve was divided into equal length segments whose end points represented the positions of the NTC. Nozzle orientation was determined using the normal vectors of an open cylinder as a reference object, to calculate values for the B and C axes. The closest point on the reference object from each NTC position was calculated to select the normal vector that most closely aligned with the intended nozzle orientation. The outcome of this process therefore defined X, Y, Z, B, and C axis values and complete extruder assembly pose, whereby pose encompasses position and orientation. Additional parameters were also incorporated into the G-code generation process, such as: extruder length, B and C offsets from the central column, and the number of equidistant points on the tool path.

The G-code was exported to text file format. As the same logic can be used to generate many wave spring geometries via 5-axis AM, only the parameter values of the developed component cluster (shown in Figure 3) would need to be modified. Each set of values can create wave springs with significantly different characteristics, which would be suitable for a range of loading conditions.

5-Axis ME Process Description

The 5-axis ME process involved a system with process settings that incorporate angles of rotation in addition to 3-axis control, it can also be referred to as 5-axis curved layer deposition. This technique allows for further improvements to the mechanical properties of AM parts by curving the layers to maintain a continuous track aligned to stress tensors, which should reduce shearing effects between adjacent track sections. It is important to note that this technique is still in its infancy with few machines capable of manufacturing in this manner (7,16).

Prior to 5-axis part manufacture a substrate was prepared in the form of a machined aluminium jig. Material was then extruded onto this structure to create 3D shells rather than the conventional '2.5D' layers. Measured lengths of masking tape were cut and successively applied to the jig to act as a substrate. The adhesive area of the tape was minimised, to aid the removal of samples from the jig, by adhering sections of tape to one another. Additional purposes of the tape were to: provide a rougher surface than the machined jig, and; provide thermal insulation between the molten polymer and the aluminium.

The 5AXISMAKER was calibrated to ensure that measured linear and rotational movements corresponded with the readings of the CNC machine controller. Relationships between filament feed rate (controlled by the A axis stepper motor), NTC speed, and extruder temperature, were identified and these parameters were optimised via 3-axis ME tests. Stepper motor speeds that controlled X, Y, Z, B, and C axis speeds were finely tuned by executing the 5-axis G-code. Each 5-axis G-code required the completion of this process, as NTC speed is dependent on movement in all axes as well as the rate of curvature change in the tool path.

To calibrate the X and Y axes, a locating pin was fastened to the machine tool collar and inserted into the corresponding hole on the top face of the jig (Fig. 7a). Once movement of the jig was constrained to the local Z axis, it was secured using a vice. This process aligned the machine Z axis with the jig Z axis, as well as zeroing X and Y coordinate values. Fine alignment was carried out by dry running the G-code with reduced motor speeds, after replacing the locating pin component with the extruder assembly.

After the sample production setup and dry running processes were complete and motor speed settings were changed to the optimised parameter values, the generated 5-axis G-code was executed. At this stage material was deposited onto the tape to form the first shell. All commands in the G-code were then followed to result in a 5-axis sample of a mechanically-optimised wave spring (as shown in Figure 7). The manufacture of each 5-axis sample required a complete repeat of this process, starting from tape application.

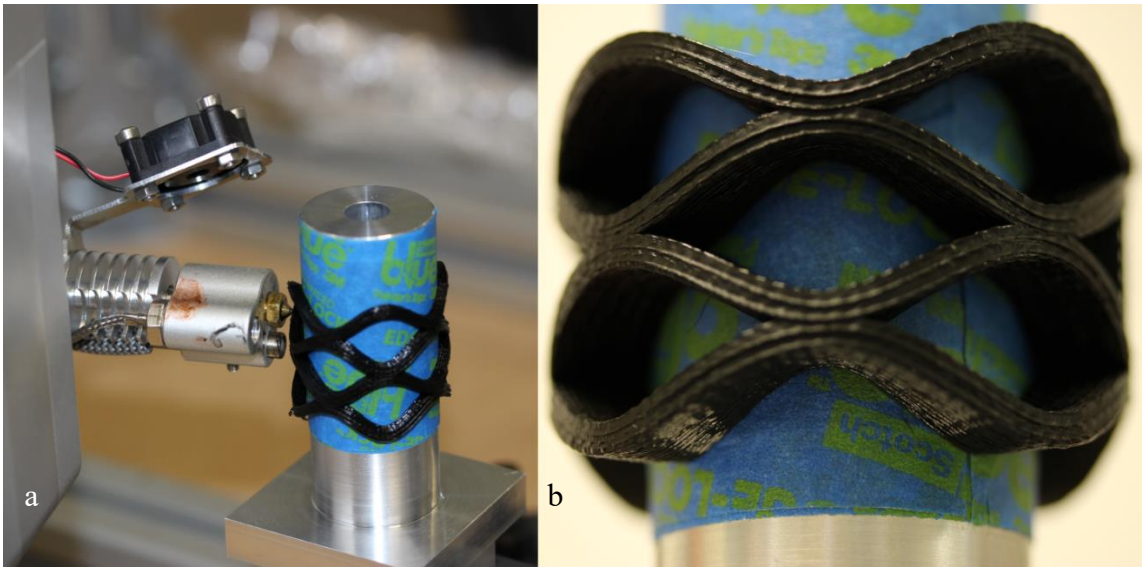

Figure 7 - A sample produced via 5-axis ME: (a) during manufacture, and (b) after manufacture

3-Axis G-code Generation

Measurements of all the 5-axis ME sample parameters (as shown in Figure 1) were taken to evaluate the differences between the manufactured geometries and the intended spring dimensions. These measurements informed the dimensions of the generated volumetric meshes that were used in the production of 3-axis ME samples. This process compensated for deviations between the 5-axis samples and their intended geometries.

An additional functionality of the component cluster developed in Grasshopper 3D was its capability to generate closed, volumetric meshes that could be sliced using MakerBot Desktop software [17]. Two sinusoidal waves were generated to function as guide geometry for a rectangular cross section to be swept along, which formed a mesh of a single wave spring layer. Similarly to the 5-axis track generation method, copies of the mesh were rotated and translated according to the number of layers and number of peaks within the layer as selected using the developed component cluster (Figure 8a).

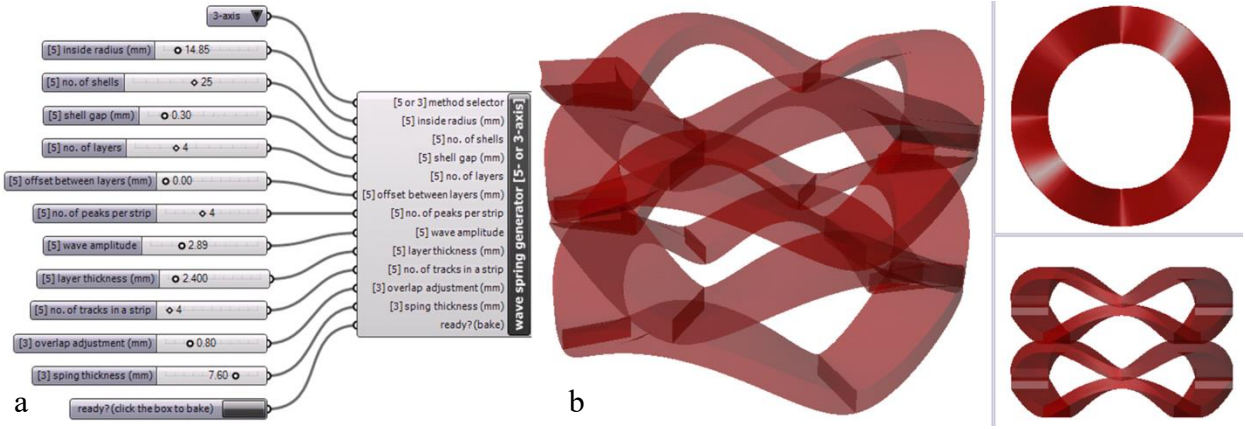

Figure 8 - Use of (a) the developed component cluster to generate (b) a closed mesh ready for G-code generation

Meshes (Figure 8b) produced by the component cluster were then exported in STL format, and imported into a mesh editing software, Autodesk Netfabb Standard 2018 [18], to remove self-intersections and output a single, volumetric mesh. The modified mesh was then imported in MakerBot Desktop software [17] where slicing parameter values were selected, by attempting to match 5-axis and 3-axis parameter values where possible. The 3D mesh was processed to form a series of 2D areas, and the associated G-code was executed to manufacture 3-axis samples (a 3-axis ME example part is shown in Figure 9).

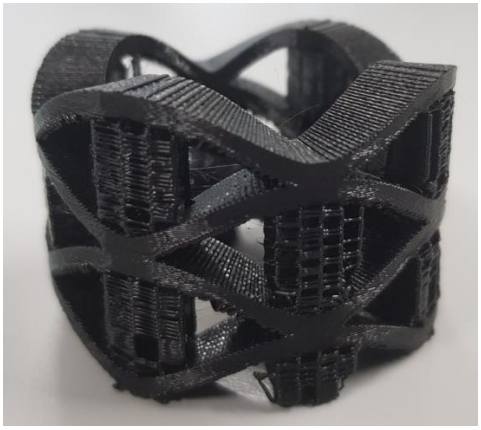

Figure 9 - A 3-axis wave spring sample, including supporting structures

The reasons for some parameter values not being identical were related to hardware variations, such as, the 5AXISMAKER and the MakerBot Replicator 2 extruder assemblies using 0.6 mm and 0.4 mm diameter nozzles, respectively. This difference resulted in a necessary dissimilarity between inter-track distances and inter-layer/shell thicknesses to maintain stable extrusion quality. Despite these differences, the measured weight was similar between sample sets.

Table 1 records the average measured values of all fabricated samples, including: the parameters shown in Figure 1, the build time, and their masses.

Table 1 - Build data for compression test samples

	Number of Layers	**Number of Waves per Layer**	**Thickness**	**Mean Diameter**	**Radial Width**	**Build Time**	**Mass**
Symbol	Z	N	t	Dm	b	N/A	N/A
Units	N/A	N/A	mm	mm	mm	min	g
5-axis	4	4	2.5	37.4	7.7	97	10.6
3-axis	4	4	2.5	37.3	7.6	110	10.7

Compression Testing

Axial compression tests were carried out using an Instron 3366 materials testing system with a 5 kN load cell and a compression speed of 2 $mm.s^{-1}$. Load and deflection were measured until failure. The compression test was conducted to demonstrate the difference in stiffness and maximum compressive load between 5-Axis and 3-Axis wave spring samples. The experimental setup can be seen in Figure 10.

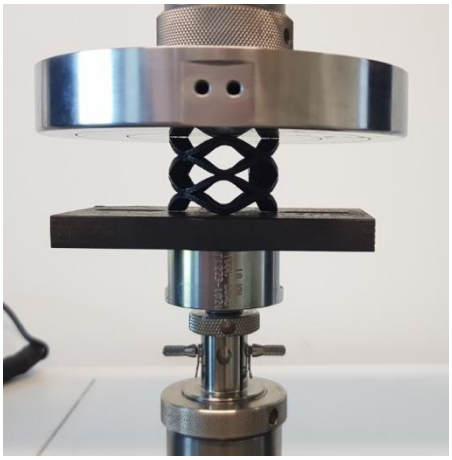

Figure 10 - Compression testing setup

Results and Discussion

The compression test results from the three, 3-Axis samples produced using the MakerBot Replicator 2 machine and three, 5-axis samples produced using the 5AXISMAKER machine were exported to an Excel spreadsheet and used to plot graphs of load against deflection (shown in Figure 11). Results from only three samples were available due to time constraints. In both the 3-axis and 5-axis conditions, it can be seen that two of the samples performed similarly to one another while a third sample was significantly different. These two significantly different samples were treated as 'outliers'. For further analysis of the results and comparisons between the conditions, average values calculated only from the two similar pairs of samples were used.

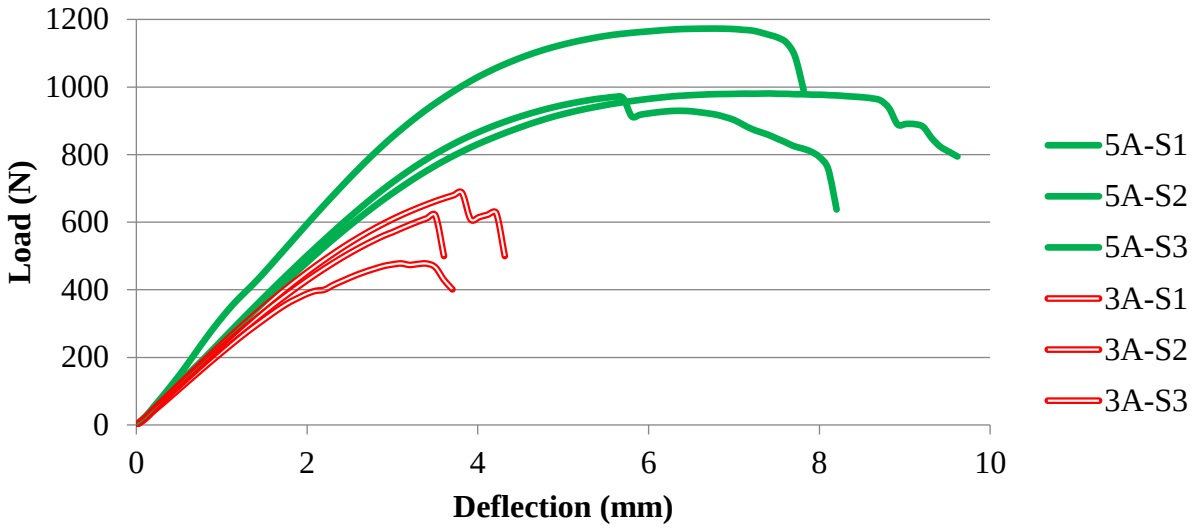

Figure 11 - A graph of force profiles generated using compression testing data

In terms of initial stiffness during small deflections (up to 1 mm), the 3-axis and 5-axis samples had very similar values of 240.3 $N.mm^{-1}$ and 248.0 $N.mm^{-1}$, respectively. This was to be expected since they were made from the same material and, under low loads, the impact of any layer-based differences in geometry or material properties would be negligible. However, above

a load value of 300 N, the load-deflection curves for the 3-axis and 5-axis samples begin to diverge and continue to do so increasingly. At a load value 600 N, the average deflection of the 3-axis samples is 0.45 mm greater than that for the 5-axis samples, i.e. they are exhibiting a lower stiffness. The precise reason for this reduction in stiffness is not yet understood but the authors suggest that it could be due the reduction in mechanical properties caused by incomplete material bonding between layers, as identified by Ahn et al (2002) [9]. In the 3-axis samples, the compressive load is transferred across many layer interfaces, whereas in the 5-axis samples, the load is largely contained within the curved shape of the layers. Hence, the anisotropic nature of the mechanical properties would have much more influence on the 3-axis samples.

The second notable difference in performance between the two sets of samples is the higher ultimate strength and increased elongation to failure exhibited by the 5-axis samples. The average maximum load values for the 3-axis and 5-axis samples were 660 N and 975 N, respectively. This can be interpreted as the 5-axis samples being 47% stronger than the 3-axis samples. Also, the average elongation to failure was 3.6 mm for the 3-axis samples and 7.3 mm for the 5-axis samples, i.e. more than a doubling in the value. However, it should be noted that there was significant variation in the elongation to failure in the 5-axis samples. Never-the-less, both the 5-axis samples performed significantly better than the 3-axis samples. These data show that aligning the material extrusion direction to the mechanical stress vectors of the wave springs has resulted in a stronger and more resilient manufacturing solution.

The third notable difference between the two sets of samples is not so apparent when looking at the recorded data, but was observed directly during the compression testing of the samples. This difference relates to the nature of the failures in the 3-axis and 5-axis samples. The 3-axis samples all failed in a brittle, catastrophic manner, with the samples seeming to 'explode' in the test apparatus. In contrast, the 5-axis samples failed in a more prolonged, stepwise manner, with the samples remaining largely intact after the tests. Examination of the samples after testing revealed that the 3-axis samples had typically failed by several cracks being propagated through all the layers at more than one region of the wave spring (see Figure 12a). Similar examination of the 5-axis samples revealed that it was more typical for a crack to have propagated through some but not all layers in a smaller number of regions (see Figure 12b). The reason for this apparent increase in plasticity from the 3-axis to the 5-axis samples is not fully understood and will be the subject of further investigations.

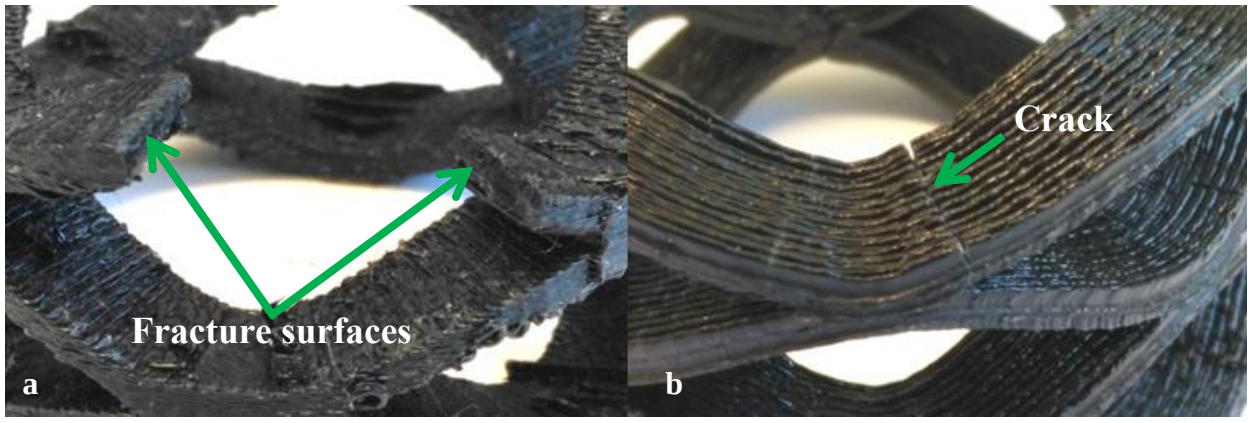

Figure 12 - A comparison of wave springs produced via (a) 3-axis and (b) 5-axis ME

As well as the samples fabricated via 5-axis ME exhibited superior mechanical properties relative to their 3-axis equivalents, the authors deemed them to be more aesthetically pleasing due the lack of the stair-stepping effect. This advantage alone is unlikely to be sufficient reason for the use of 5-axis ME, due to the complexity of the process, predominantly: G-code generation and machine and jig setup processes.

Although the design of the developed component cluster (Figure 3) allows for the most time-consuming G-code generation stage, the creation of the tool path, to be completed automatically, the cluster is limited to only producing a continuous track that describes a wave spring. One of the main appeals of 3-axis ME is the relative simplicity of the G-code generation process [19], as almost any volumetric mesh can be processed entirely automatically. For 5-axis ME to become a more viable option of manufacturing parts, with optimised mechanical properties, the tool path creation process should be more automated. 3-axis ME strategies and machines that provide options of optimising mechanical properties of parts typically rely on increasing feature thicknesses or reinforcing layers with heterogeneous materials [20], respectively. To minimise the differences between the conventional G-code generation process for ME, the authors propose that volumetric meshes are similarly imported into a virtual environment, and at that point the user, or an additional automated process, determines the ME direction. This process may also incorporate jig production processes if required. To compare the above described software approach with the process followed to produce a single wave spring highlights the gaps that need to be addressed for the adoption of 5-axis ME.

Conclusions

This work has demonstrated that 5-axis ME can be used as an effective means to generate high quality polymer parts. The samples created by the 5-axis process had improved surface finish, higher strength and a non-catastrophic failure mechanism. The results from the compression testing showed a 47% increase in strength, comparable to the 40% increase seen by Sinanemi et al in their experiments with curved layer ME [7]. This was due largely to the material extrusion tracks being aligned with the stress tensors experienced by the wave spring samples, a particularly novel aspect of this work. Deflection to failure was also increased significantly. The authors recognise that these results are tentative in nature since the sample size was small and a there was marked variability in the results. Never-the-less, they do indicate that 5-axis ME is a promising direction to pursue.

The ‘downside’ of 5-axis ME is the added complexity of the equipment (including build set-up) and the additional time and effort needed to generate tool paths compared to those required for 3-axis ME. For the samples created for this paper, numerous steps were involved using several different software packages. This would be an unrealistic process chain for design and manufacturing engineers to follow in a commercial environment.

At time of writing, further samples were being built for the purpose of confirming the initial compression test results. Finite element analysis (FEA) will then be used to gain a better understanding of the failure modes and the reason for the apparent increase in plasticity in the 5-axis samples. Looking further ahead, a new project has been started with the aim of developing

an industry-ready 5-axis ME system and associated software to facilitate automated generation of tool paths from design and FEA data [21].

Acknowledgements

This work was partly funded through the Engineering and Physical Sciences Research Council (Additive Manufacturing and 3D Printing Centre for Doctoral Training) and the European Commission (AMa-TUC Project 691787). Thanks also go to 5AXISWORKS Ltd for their help in programming and calibrating the 5-axis manufacturing system. Additional thanks go to the technical staff at Loughborough Design School for providing key equipment that enabled timely sample production.

References

[1] N. Turner, B., Strong, R., & A. Gold, S. (2014). A review of melt extrusion additive manufacturing processes: I. Process design and modeling. Rapid Prototyping Journal, 20(3), 192-204. doi: 10.1108/rpj-01-2013-0012

[2] Gao, W., Zhang, Y., Ramanujan, D., Ramani, K., Chen, Y., & Williams, C. et al. (2015). The status, challenges, and future of additive manufacturing in engineering. Computer-Aided Design, 69, 65-89. doi: 10.1016/j.cad.2015.04.001

[3] Yang, S., & Zhao, Y. (2015). Additive manufacturing-enabled design theory and methodology: a critical review. The International Journal Of Advanced Manufacturing Technology, 80(1-4), 327-342. doi: 10.1007/s00170-015-6994-5

[4] Sood, A., Ohdar, R., & Mahapatra, S. (2012). Experimental investigation and empirical modelling of FDM process for compressive strength improvement. Journal Of Advanced Research, 3(1), 81-90. doi: 10.1016/j.jare.2011.05.001

[5] Zhang, Y., & Chou, K. (2008). A parametric study of part distortions in fused deposition modelling using three-dimensional finite element analysis. Proceedings Of The Institution Of Mechanical Engineers, Part B: Journal Of Engineering Manufacture, 222(8), 959-968. doi: 10.1243/09544054jem990

[6] Wang, T., Xi, J., & Jin, Y. (2006). A model research for prototype warp deformation in the FDM process. The International Journal Of Advanced Manufacturing Technology, 33(11-12), 1087-1096. doi: 10.1007/s00170-006-0556-9

[7] Singamneni, S., Roychoudhury, A., Diegel, O., & Huang, B. (2012). Modeling and evaluation of curved layer fused deposition. Journal Of Materials Processing Technology, 212(1), 27-35. doi: 10.1016/j.jmatprotec.2011.08.001

[8] Kubalak, J., Wicks, A., & Williams, C. (2017). Using multi-axis material extrusion to improve mechanical properties through surface reinforcement. Virtual And Physical Prototyping, 13(1), 32-38. doi: 10.1080/17452759.2017.1392686

[9] Ahn, S., Montero, M., Odell, D., Roundy, S., & Wright, P. (2002). Anisotropic material properties of fused deposition modeling ABS. Rapid Prototyping Journal, 8(4), 248-257. doi: 10.1108/13552540210441166

[10] Cantrell, J., Rohde, S., Damiani, D., Gurnani, R., DiSandro, L., & Anton, J. et al. (2017). Experimental characterization of the mechanical properties of 3D-printed ABS and polycarbonate parts. Rapid Prototyping Journal, 23(4), 811-824. doi: 10.1108/rpj-03-2016-0042

[11] PLA. (2017). Retrieved from http://usglobalimages.stratasys.com/Main/Files/Material_Spec_Sheets/MSS_FDM_PLA_0117b_Web.pdf
[12] Newfangled Solutions. (2006). Mach3 (Version R3.043) [Windows]. Livermore Falls, Maine.
[13] 5AXISWORKS. (2018). 5xMonkey [Windows].
[14] Rutten, D. (2009). Grasshopper 3D (Version 0.9.0076) [Windows]. Roger de Flor, Barcelona, Spain: Robert McNeel and Associates.
[15] Robert McNeel & Associates. (2017). Rhinoceros 3D (Version 5.14.522.8390) [Windows]. Roger de Flor, Barcelona, Spain.
[16] Chakraborty, D., Aneesh Reddy, B., & Roy Choudhury, A. (2008). Extruder path generation for Curved Layer Fused Deposition Modeling. Computer-Aided Design, 40(2), 235-243. doi: 10.1016/j.cad.2007.10.014
[17] MakerBot. (2018). MakerBot Desktop (Version 3.10.1) [Windows]. New York City, New York.
[18] Autodesk. (2017). Autodesk Netfabb Standard 2018 (Version 1608) [Windows]. San Rafael, California.
[19] Steenhuis, H., & Pretorius, L. (2016). Consumer additive manufacturing or 3D printing adoption: an exploratory study. Journal Of Manufacturing Technology Management, 27(7), 990-1012. doi: 10.1108/jmtm-01-2016-0002
[20] Dickson, A., Barry, J., McDonnell, K., & Dowling, D. (2017). Fabrication of continuous carbon, glass and Kevlar fibre reinforced polymer composites using additive manufacturing. Additive Manufacturing, 16, 146-152. doi: 10.1016/j.addma.2017.06.004
[21] DiCoMI Project. (2018). Retrieved from http://www.dicomi.eu/